

Adsorption States and Photochemistry of NO₂ Adsorbed on Au(111)Shinri Sato,^{*,†} Takehito Senga, and Masahiro Kawasaki

Catalysis Research Center and Graduated School of Environmental Earth Science, Hokkaido University, Sapporo 060-0811, Japan, and Department of Molecular Engineering, Kyoto University, Kyoto 606-8501, Japan

Received: March 1, 1999; In Final Form: April 14, 1999

The photochemistry of NO₂ adsorbed on an Au(111) surface has been investigated at <120 K in an ultrahigh vacuum system. The adsorption states of adsorbates were characterized by thermal desorption spectroscopy and IR reflection absorption spectroscopy (IRAS). The adsorption of NO₂ leads to formation of chemisorbed NO₂, N₂O₄ (*D*_{2h} symmetry) in direct contact to the surface, and well-ordered N₂O₄ (*D*_{2h} symmetry) physisorbed on these species without formation of other unstable N₂O₄ isomers. While the former two species undergo neither photodissociation nor photodesorption, physisorbed N₂O₄ is dissociated to NO₂, NO, and adsorbed atomic oxygen under irradiation at $\lambda < 430$ nm. IRAS showed that no intermediate species such as adsorbed NO₂ or NO₃ were formed during N₂O₄ photolysis. The photodissociation cross section of physisorbed N₂O₄ at 350 nm was found to be 5.6×10^{-19} cm², which is close to the absorption cross section of gas-phase N₂O₄. Wavelength dependence of the cross section is very similar to the absorption spectrum of N₂O₄ adsorbed on LiF at 68 K. Physisorbed N₂O₄ photolysis is inhibited significantly when the Au surface is covered with a thin water ice film, suggesting that the photolysis is enhanced by metal substrate photoexcitation or electron transfer from the substrate to the adsorbates.

1. Introduction

The photochemistry of molecules adsorbed on a solid surface has received increasing attention in recent decades since it provides information for adsorbate–surface interactions, including energy and charge transfer, dynamics, and kinetics.¹ For the surface photochemistry of NO₂, Hasselbrink et al.² studied the UV laser-induced desorption of NO from submonolayer NO₂ (actually present as N₂O₄) adsorbed on top of a NO saturated Pd(111) surface. They found two different desorption channels using laser-induced fluorescence, one characterized by non-thermal state populations, and one showing accommodation to the surface. They also carried out polarization experiments, concluding that the photodissociation is initiated by excitation of metal electrons rather than direct photoabsorption by the adsorbate. Dixon-Warren et al.³ investigated, on the other hand, the photodissociation of NO₂ (N₂O₄) adsorbed on LiF(001), which leads to desorption of NO and NO₂. They found two different translational energy distributions for NO, and NO₂-coverage-dependent translational energy for NO₂. Although they characterized reaction intermediates using IR transmission spectroscopy, its sensitivity was low, and the spectral region was limited to >1500 cm⁻¹ due to cutoff of the LiF substrate.

While the motivation of these studies stems from the dynamics of a surface photochemical reaction, the heterogeneous reactions of NO_x species on water ice surfaces have attracted attention in recent years from an environmental chemistry point of view, since the surfaces of polar stratospheric clouds, which mainly consist of water ice, have been implicated as playing a central role in the photochemical mechanism responsible for the yearly occurrence of the ozone hole.^{4–6} Rieley et al.⁷ investigated the photochemistry of N₂O₄ adsorbed on ice films formed on a Cu foil using IR reflection absorption spectroscopy

(IRAS) for characterization of the adsorption states. They observed the photodesorption of NO₂ under near-UV irradiation. Since the wavelength dependence of the NO₂ yield was comparable to the gas-phase absorption cross section for N₂O₄, they concluded that the photochemistry of N₂O₄ on ice is not significantly different to that of gas-phase N₂O₄. They also studied photodesorption dynamics of NO₂ from N₂O₄ adsorbed on ice surfaces.⁸

Since the photochemical properties of adsorbates are significantly affected by their adsorption states including orientations, in situ characterization of adsorbates by surface spectroscopy is essential to deeper insight into a mechanism of surface photochemistry. We have used IRAS for in situ observation of surface species before and during surface photoreactions.⁹ Although a substrate for IRAS study is usually a smooth metal with a high reflection coefficient, various thin films coated on such a metal can also be used. A metal substrate used for surface photochemistry is required to be as inert as possible in order to minimize a change in electronic states due to adsorbates–surface interactions. We have used an Au single crystal as a substrate, since Au is known to be most inactive among transition metals.⁹ In the present paper we report the photochemistry of NO₂ adsorbed on an Au(111) surface. The adsorption states of NO₂ on a clean Au(111) surface were already investigated by Koel and co-workers^{10,11} using HREELS, IRAS, and TPD. They found that NO₂ is adsorbed molecularly on the surface to form a surface chelate at <170 K (we refer to this species as chemisorbed NO₂), and over the chemisorbed NO₂ layer, NO₂ is physisorbed as N₂O₄. They also found that the chemisorbed NO₂ reacts readily with gas-phase NO to form N₂O₃ on the surface. We report in the present paper the photochemistry of NO_x species on an Au(111) surface with the detailed characterization of adsorbates by IRAS and TPD.

[†] E-mail: shinri@cat.hokudai.ac.jp. Fax: +81-11-709-4748.

2. Experimental Section

The experimental apparatus used was similar to that described previously.⁹ An Au(111) single crystal (12 mm in diameter, 1.5 mm thick, 99.999% purity) was purchased from Mateck. The sample was cleaned by repeating Ar ion sputtering and annealing at 800 K. Ozone was sometimes used for surface cleaning.

Thermal desorption spectra (TDS) of adsorbates were obtained using a quadrupole mass spectrometer (ANELVA AQA-200), which is located at ca. 35° with respect to the substrate surface normal. Since NO₂ undergoes fragmentation during ionization to produce NO⁺, the mass analysis of a mixture of NO and NO₂ needs correction for the contribution of NO⁺ from NO₂. The pattern coefficients of NO₂ were determined using the TDS of NO₂ from adsorbed N₂O₄. For IRAS measurements, the IR beam from FTIR (BIO-RAD FTS-155) was introduced into the chamber through a BaF₂ window, the cutoff wavelength of which is around 900 cm⁻¹. The incident angle of the IR beam was ~85°, and a wire grid polarizer was used to select p-polarized light, since only p-polarized light is effective for IRAS.^{11,12} The paths of the IR beam were purged with dry air to reduce the effects of moisture. IRA spectra were recorded with 4 cm⁻¹ resolution and 200 scans.

The light source was a paraboloidal-reflector Xe lamp (ILC LX300UV, 300 W), which was monochromatized by a grating monochromator (RITSU MC-20L) and focused by a quartz lens onto the sample through an MgF₂ window. A water filter (20 cm long) was placed in front of the lamp to remove radiative heat. Incident photon flux into the chamber was measured using chemical actinometry. When intense irradiation was necessary, a band-pass filter (230–400 nm, Toshiba UV-D33S) was used instead of the monochromator. The substrate temperature was initially elevated at ca. 1 K/min and leveled off at ca. 100 K in this case. To reduce light intensity, neutral-density filters (Toshiba) were used.

NO₂ was stored in a glass reservoir in the presence of an excess of O₂ to prevent its decomposition to NO and O₂ during storage. The gas mixture was frozen at 77 K and O₂ was pumped away before use. Since NO₂ was decomposed to some extent in the gas handling system, the inner wall of the stainless steel pipe was passivated by exposing a relatively high pressure of NO₂ or O₃ for a prolonged time. Gases were introduced into the chamber through a nozzle, the end of which was ca. 1 cm away from the substrate. A pulsed valve (General Valve) was used to control exposures of gases to the surface.

3. Results and Discussion

3.1. Characterization of Adsorption States. 3.1.1. TPD Experiments. Figure 1 shows thermal desorption spectra from NO₂ adsorbed on the Au(111) surface at 92 K. The desorption peak centered at 206 K (γ peak) is attributed to the desorption of NO₂ chemisorbed on the surface and the one at 132 K (α peak) to NO₂ physisorbed on chemisorbed NO₂. A small peak centered at 152 K (β peak) was also observed by Bartram and Koel,¹⁰ but not characterized. We attribute this peak to N₂O₄ adsorbed on the vacant Au surface remained after NO₂ chemisorption based on our IRAS results. The fact that the β peak mainly comprises NO indicates that this N₂O₄ species undergoes thermal decomposition during TPD. Bartram and Koel¹⁰ reported that the exposure necessary for the saturation coverage of chemisorbed NO₂ was ca. 2.0 langmuirs (1 langmuir = 10⁻⁶ Torr·s), and the sticking probability was close to unity for both chemisorbed NO₂ and physisorbed N₂O₄. On the basis of their results, we take a saturation coverage as 1 monolayer (ML). As seen in Figure 1, the NO₂⁺/NO⁺ ratio for the γ peak is

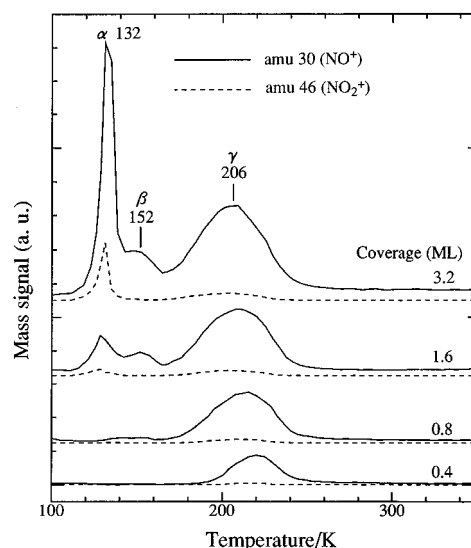


Figure 1. Thermal desorption spectra (TDS) from NO₂ adsorbed on an Au(111) surface as a function of coverage. The temperature ramp was 4 K/s.

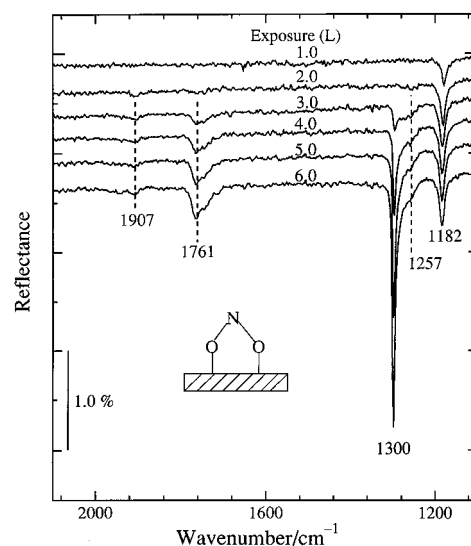


Figure 2. IRA spectra of NO₂ adsorbed on an Au(111) surface at 93 K as a function of exposure. The inset illustrates the adsorption state of chemisorbed NO₂.

smaller than that for the α peak, indicating that not only NO₂ but also NO was desorbed from chemisorbed NO₂. Corrected with the sensitivity ratio of NO to NO₂ in the mass analysis (ca. 32 in our case), the γ peak was found to involve 26% of NO in case of Figure 1 (temperature ramp of 4 K/s). The NO ratio in γ peak increased with decrease in the temperature ramp of TPD. For the heating rate of 1 K/s, 52% of the desorbed gases were NO. These results show that the desorption of NO₂ competes with decomposition to NO and adsorbed atomic oxygen. The destination of adsorbed oxygen will be discussed later.

3.1.2. IRAS Measurements. Figure 2 shows IRA spectra of NO₂ adsorbed on the Au(111) surface at 92 K as a function of exposure. Band assignments of adsorbed NO₂ and N₂O₄ are given in Table 1 together with those by Koel and co-workers^{10,11} and Koch et al.¹² Because IRAS is insensitive to the vibrational modes parallel to the surface (surface selection rule),^{13,14} the asymmetric stretching of chemisorbed NO₂, which is parallel to the surface, cannot be detected by IRAS. A similar surface selection rule has also been reported for HREELS.¹⁵ The

TABLE 1: Vibrational Frequencies (cm⁻¹) and Assignments of Adsorbed NO₂ and N₂O₄ on Au Surfaces^a

mode	chemisorbed NO ₂			adsorbed N ₂ O ₄			
	HREELS ^b	IRAS ^c	IRAS ^d	HREELS ^b	IRAS ^c	IRAS ^e	IRAS ^d
δ(NO ₂)	800	805	n.d.	770	783	785	n.d.
ν _s (NO ₂)	1180	1178	1182	1280	1298	1301	1257 (first layer) 1300 (multilayer)
ν _a (NO ₂)	1180		(IRAS inactive)	1755	1735 1760	1750	1761

^a δ, bending; ν, stretching. n.d., no data due to the cutoff of the CaF₂ windows. ^b Reference 10. ^c Reference 11. ^d This work. ^e Reference 12; this N₂O₄ species was formed on an uncleaned Au surface, on which chemisorbed NO₂ is not produced.

complete absence of the strong asymmetric stretching band of NO₂ around 1600 cm⁻¹ indicates the absence of other NO₂ species on the surface. The weak band at 1907 cm⁻¹ is attributable to the N–O stretching of N₂O₃ formed by a reaction of chemisorbed NO₂ with gas-phase NO,^{10,11} since a trace amount of NO was produced by decomposition of NO₂ during injection. Adsorbed N₂O₃ also exhibits a NO₂ symmetric stretching band at 1274 cm⁻¹. The bands at 1257, 1300, and 1761 cm⁻¹ are attributed to condensed N₂O₄ with D_{2h} symmetry as assigned previously.^{12,16,17} It is known that some unstable isomers of N₂O₄ are formed in a low-temperature inert matrix and in a condensed phase of NO₂.^{18–24} Among such isomers, D-isomers, O=N–O–NO₂, may play an important role in the photochemistry of condensed N₂O₄, because D-isomers can be thermally converted into nitrosonium nitrate, NO⁺NO₃⁻,^{21–24} and undergo more rapid photolysis than N₂O₄(D_{2h}) in an Ar matrix.²⁵ D-isomers exhibit IR bands at 1290–1310 cm⁻¹ (NO₂ symmetric stretching), 1630–1645 cm⁻¹ (NO₂ asymmetric stretching), and 1820–1830 cm⁻¹ (N=O stretching) in IRAS as well as in transmission IR.^{18–24} Although the band at 1300 cm⁻¹ in Figure 2 is very close to the NO₂ symmetric stretching of D-isomers, any other bands attributable to D-isomers were not observed in our experiments. No change was observed in IRAS after adsorbed N₂O₄ was annealed at 110 K. These results indicate that the 1300 cm⁻¹ band is not due to D-isomers.

In our IRAS measurements, the 1257 cm⁻¹ band grew only at low coverages (<2 ML), and therefore, this band could be assigned to N₂O₄ adsorbed directly on Au surface (we refer to this species as first-layer N₂O₄). When the substrate temperature was elevated after NO₂ adsorption, the 1257 cm⁻¹ band remained even after disappearance of the 1300 cm⁻¹ band and finally disappeared at around 160 K. Therefore, the β peak in TDS is attributable to first-layer N₂O₄. The IRA spectrum of first-layer N₂O₄ resembles the IR transmission spectrum of gas-phase N₂O₄, in which the band intensities of symmetric and asymmetric NO₂ stretching are comparable, indicating random configuration of first-layer N₂O₄. NO₂ is physisorbed (condensed) on both chemisorbed NO₂ and first-layer N₂O₄ to form multilayer N₂O₄. For multilayer N₂O₄, the O–N–O symmetric stretching band, the vibrational mode of which is parallel to the C₂ axis (N–N bond axis), grows solely with increasing coverage as shown in Figure 2. Similar results have been obtained for the Au foil¹⁶ and the water ice⁷ surfaces as well as for the chemisorbed NO₂/Au(111) system.¹¹ Based on the surface selection rule of IRAS,^{13,14} we can conclude that multilayer N₂O₄ is aligned preferentially with the C₂ axis perpendicular to the surface.

The sticking probability of NO₂ to form multilayer N₂O₄ was significantly attenuated at >110 K, although those for chemisorbed NO₂ and first-layer N₂O₄ were still close to unity. At 120 K the sticking probability to form multilayer N₂O₄ was about one-tenth of that observed at 90 K.

3.2. Photochemistry of NO_x Species. 3.2.1. Photodissociation Products. UV irradiation (230–400 nm) of chemisorbed

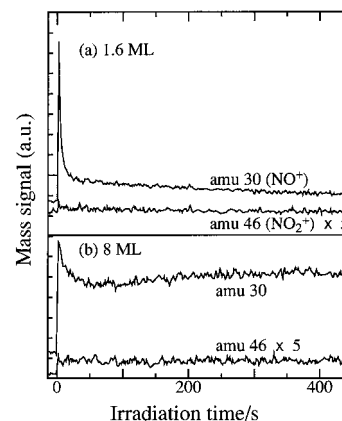


Figure 3. Photodesorption of NO₂ and NO from NO₂ adsorbed on an Au(111) surface at 92 K. A band-pass filter (UV-D33S, 230–400 nm) was used for irradiation.

NO₂, which was formed by NO₂ adsorption at 160 K, led to no evolution of gases. IRAS showed no change in the 1184 cm⁻¹ band intensity even after prolonged irradiation. Thus, electric quenching is very rapid in the photodissociation of chemisorbed NO₂ due to bonding formation of the two oxygen atoms with the Au surface.¹⁰

UV irradiation of multilayer N₂O₄ led to desorption of NO and NO₂ without formation of any other species. Figure 3 shows time-dependent gas evolution during irradiation at 92 K. At low coverages, a sharp spike of NO desorption was observed at the beginning of illumination. This spike was found to arise from rapid photodissociation of adsorbed N₂O₃ in a separate experiment, in which adsorbed N₂O₃ alone was illuminated. The details of N₂O₃ photodissociation will be reported elsewhere. At higher coverages, the initial rapid desorption of NO was significantly suppressed. After complete decomposition of N₂O₃, the photodesorption of NO and NO₂ almost leveled off. A slight increase in NO yield after 1 min irradiation may be due to destruction of the ordered N₂O₄ layer, since the photodissociation of ordered N₂O₄ would undergo more rapid quenching than that of disordered one. The photodesorption yields of NO₂ and NO from multilayer N₂O₄ were determined as a function of coverage after the decomposition of N₂O₃ was completed (Figure 4). The NO₂/NO ratio was nearly unity at low coverages and increased with increasing coverage. The NO₂/NO ratio in the present system is greater than that reported for the N₂O₄/NO/Pd(111) system,² where at least 90% of the desorbed molecules were NO under 193-nm radiation. The NO₂/NO ratio in adsorbed N₂O₄ photolysis was found to be sensitive to surface species preadsorbed on the substrate. For instance, when the Au surface was covered with *n*-decane (~1 ML), the photodesorbed molecules from the physisorbed N₂O₄ layer (1 ML) were predominantly NO at 350 nm.²⁶ The NO₂/NO ratio in the present system also depended upon substrate temperature as shown in Figure 5. In this experiment NO₂ was adsorbed at <96 K, and then the substrate was heated to each temperature, followed by

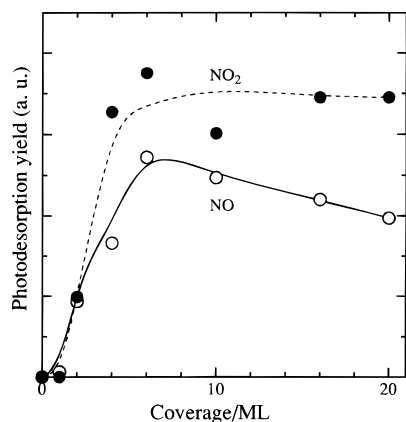


Figure 4. Photodesorption yields of NO_2 and NO as a function of coverage at 93 K. A band-pass filter (UV-D33S, 230–400 nm) was used for irradiation.

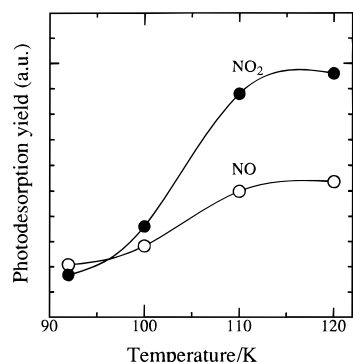


Figure 5. Temperature dependence of the photodesorption yields of NO_2 and NO . The total coverage of adsorbed NO_2 was 3.6 ML. A band-pass filter (UV-D33S, 230–400 nm) was used for irradiation.

measurement of photodesorbing species. N_2O_4 was not desorbed at any temperature. The temperature dependence for NO_2 photodesorption was more remarkable than for NO desorption; NO_2 yield at >110 K was more than 4 times greater than that at 95 K, while the increase in NO yield was about 2-fold. Because the photochemical yield is independent of temperature, this result indicates that some thermal processes significantly reduce the photodesorption yield at <110 K. NO_2 yield could be suppressed by the back reaction, $2\text{NO}_2(\text{ad}) \rightarrow \text{N}_2\text{O}_4(\text{ad})$, while NO yield could be suppressed by a reaction such as $\text{NO} + \text{O}(\text{a}) \rightarrow \text{NO}_2(\text{a})$.

Neither atomic nor molecular oxygen was detected in the gas phase during multilayer N_2O_4 photolysis, indicating that adsorbed atomic oxygen or oxygen-containing species must be formed on the surface. Careful examination of IRA spectra after prolonged irradiation led us to conclude that any new NO_x species such as NO_3 or N_2O_5 were not produced by the photolysis. We have recently investigated the reactivities of ozone and atomic oxygen adsorbed on $\text{Au}(111)$ surface, which was produced from adsorbed ozone, and found that adsorbed N_2O_4 does not react with O or O_3 adsorbed on Au surface at <100 K while NO reacts with O to form $\text{NO}_2(\text{a})$ and $\text{N}_2\text{O}_4(\text{a})$.²⁶ For the NO -covered $\text{Pd}(111)$ surface, Hasselbrink et al.² reported no formation of adsorbed oxygen after irradiation and ascribed this result to a reaction of adsorbed atomic oxygen with preadsorbed NO . They found, however, adsorbed atomic oxygen when N_2O_4 was directly adsorbed on a clean $\text{Pd}(111)$ surface.²

To detect adsorbed oxygen in our system, TPD was carried out after the photodissociation of multilayer N_2O_4 . As shown in Figure 6, O_2 desorption was observed at around 507 K in

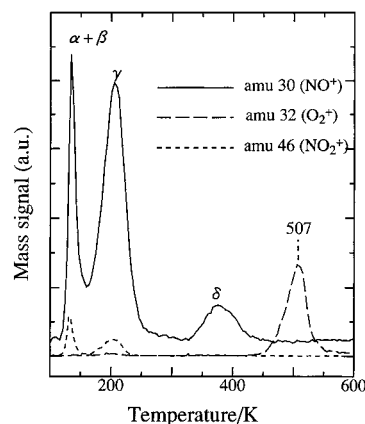


Figure 6. TDS after 8 min photolysis of NO_2 (2 ML) adsorbed on an $\text{Au}(111)$ surface at 93 K. A band-pass filter (UV-D33S, 230–400 nm) was used for irradiation. The origin of the δ peak is not clear, but IRAS showed that the species giving the δ peak is not present on the front surface of the substrate.

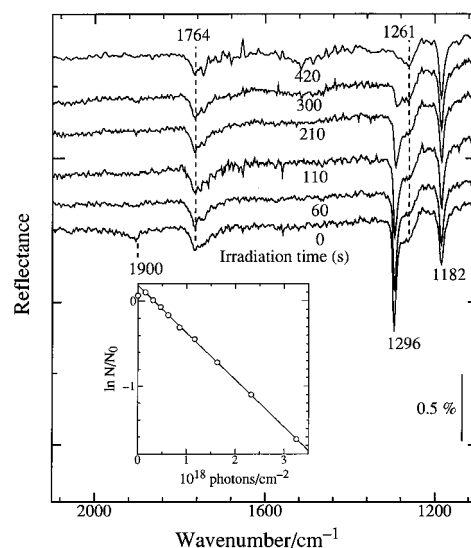


Figure 7. Change in IRA spectrum during the photolysis at 350 nm. The initial coverage of adsorbed NO_2 was 2.5 ML. The inset is the semilogarithmic plots of the residual amount of multilayer N_2O_4 for determination of a cross section (see text).

TPD, indicating the formation of adsorbed atomic oxygen during the photolysis. While it is widely known that Au surface is unable to adsorb O_2 , Canning et al.²⁷ reported that atomic oxygen produced by a hot Pt filament is promptly adsorbed on Au surfaces at room temperature to form oxide layer, from which O_2 is desorbed at >500 K. It is therefore reasonably concluded that atomic oxygen produced by the photodissociation of multilayer N_2O_4 remains on the Au surface without reacting with the NO_x species. In passing, Figure 1 shows that chemisorbed NO_2 is partly decomposed to NO without O_2 evolution during TPD, but O_2 desorption was observed at 507 K, when the adsorption–desorption cycle of chemisorbed NO_2 was repeated a few times at <400 K to accumulate atomic oxygen on the surface.

3.2.2. Photodissociation Cross Sections. Figure 7 shows changes in the IRAS bands of chemisorbed NO_2 , N_2O_3 , and first-layer and multilayer N_2O_4 (2.5 ML total coverage) during irradiation at 350 nm. Within the first 1 min of illumination, the 1900 cm^{-1} band assigned to adsorbed N_2O_3 disappears due to its rapid photodecomposition, while the 1182 cm^{-1} band (chemisorbed NO_2) increases slightly corresponding to the conversion of N_2O_3 into chemisorbed NO_2 . The 1296 cm^{-1} band

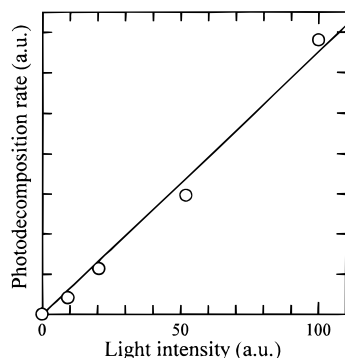


Figure 8. Light intensity dependence of the decreasing rate of multilayer N₂O₄ under irradiation at 350 nm. Neutral-density filters were used to control light intensity. The initial coverage of adsorbed NO₂ was 2.5 ML, and the substrate temperature 92 K.

(multilayer N₂O₄) also increased slightly upon illumination, but the reason for this is obscure at the present. The 1261 and 1182 cm⁻¹ bands (first-layer N₂O₄ and chemisorbed NO₂) remain unchanged even under prolonged irradiation. This result indicates that the quenching of photoexcited states is significant for these species due to its direct contact with the surface. The decay of the 1296 cm⁻¹ band absorbance assigned to the NO₂ symmetric stretching of multilayer N₂O₄ follows a simple exponential law. This indicates that the amount of residual multilayer N₂O₄, N , is given as¹

$$N = N_0 \exp(-\sigma n_{hv}) \quad (1)$$

where N_0 is the initial amount of multilayer N₂O₄, σ the cross section, and n_{hv} the number of photons irradiated. From the absorbance of the NO₂ symmetric stretching at 1296 cm⁻¹, N/N_0 was determined. The inset of Figure 7 shows the plots of $\ln N/N_0$ versus n_{hv} . The cross section is determined from the slope to be 5.6×10^{-19} cm². This value is larger than the cross section, 1.3×10^{-19} cm², determined for the N₂O₄/NO/Pd(111) system² at 351 nm, but close to the absorption cross section, 5.7×10^{-19} cm², of gas-phase N₂O₄ at 350 nm.^{28,29} Thus, the quantum yield of the present system is found to be remarkably high. Light intensity dependence of the photodissociation cross section of multilayer N₂O₄ was measured at 350 nm with neutral-density filters. The decreasing rate of the 1296 cm⁻¹ band absorbance was virtually proportional to light intensity as shown in Figure 8. Wavelength dependence of the photodissociation cross section is shown in Figure 9. Similar wavelength dependence of the photodissociation cross section was reported for the N₂O₄/NO/Pd(111) system using 248, 308, and 351-nm lasers.² The inset of the figure shows the absorption spectra of gas-phase N₂O₄²⁸ and NO₂ (N₂O₄) adsorbed on LiF at 68 K.³⁰ The observed wavelength dependence of the cross section is very similar to the absorption spectrum of N₂O₄ adsorbed on LiF, except for the absorption edge. Although this similarity seems to imply direct photoabsorption by multilayer N₂O₄, there exists a possibility of photoexcitation of the Au surface.

To examine substrate photoexcitation, the photodissociation of adsorbed N₂O₄ was carried out on a thin film of water ice (~5 ML) formed on the Au surface. Gas-phase water was adsorbed at 130 K in order to minimize surface roughness and grain boundaries. Although photoinduced electrons were found to pass through water layers formed on a Ni(111) surface at 50 K, 5 ML water layers were enough to prevent electron transmission.³¹ IRAS showed that NO₂ is adsorbed on the ice film as N₂O₄, which is very similar to multilayer N₂O₄ on the Au surface. Figure 10 shows the time-dependent mass signals

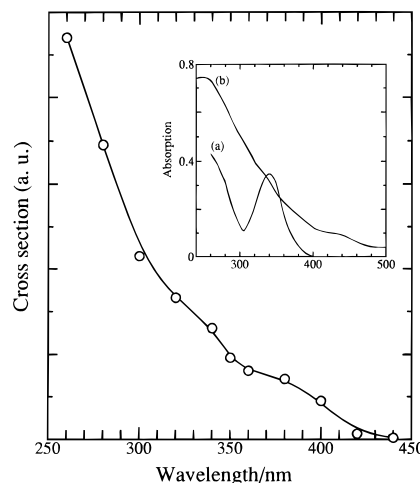


Figure 9. Wavelength dependence of the photodissociation cross section of multilayer N₂O₄ at 93 K. The total coverage of adsorbed NO₂ was 3 ML. The inset shows the absorption spectra of (a) gas-phase N₂O₄²⁷ and (b) N₂O₄ adsorbed on LiF at 68 K.²⁸

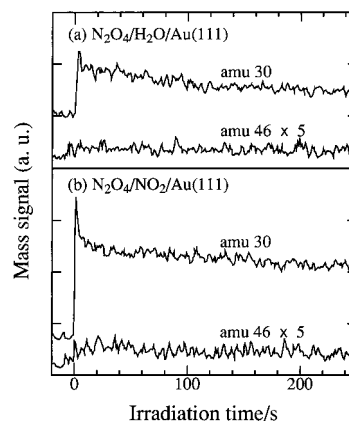


Figure 10. Effect of a thin ice film (~5 ML) covering the Au(111) surface on the photodesorption of NO₂ and NO from adsorbed NO₂ (2.5 ML) at 93 K under irradiation at 350 nm: (a) on the ice film and (b) on the bare Au surface.

of photodesorbing gases from N₂O₄ adsorbed on the ice surface at 92 K together with the corresponding profile for the N₂O₄/NO₂/Au(111) system. For Figure 10b the initial sharp peak of NO desorption is due to the rapid photodecomposition of N₂O₃ adsorbed on Au(111) surface. From comparison of the two photodesorption profiles, we are confident that the photodesorption yields of NO and NO₂ from multilayer N₂O₄ on the Au(111) surface are greater than those from N₂O₄ adsorbed on the ice surface. IRAS observation also confirmed greater photolysis rate of N₂O₄ on the Au surface than on the ice surface. Since the surface of an insulator such as water ice is thought to have little effect on the yield of a surface photoreaction, this result suggests the enhancement of N₂O₄ photodissociation by effects of the Au surface.

3.2.3. Mechanism of Multilayer N₂O₄ Photodissociation.

Whether or not a surface photoreaction on a metal surface occurs by substrate photoexcitation can be determined by a polarization probe method, in which the polarization-dependent yield is measured as a function of the incident angle of light.¹ Hasselbrink et al.² applied this method to the N₂O₄/NO/Pd(111) system at 193 and 248 nm and concluded that the photoabsorption by the metal is the dominant primary step in the photodissociation. The enhancement of photoreactions on metal surfaces is usually ascribed to photoelectron capture by adsorbed molecules. Photoelectron emission from Pd, however, could not occur at

>220 nm, since the work function of clean Pd is 5.6 eV. Hasselbrink et al.,² therefore, assumed that electrons created by light energies less than the work function penetrate the potential barrier at the metal/adsorbate interface through tunneling and induce the photolysis. The optical absorption coefficient of Pd changes, however, only by a factor of 1.5 in the wavelength region from 351 to 193 nm. This change, therefore, cannot explain the observed pronounced increase (more than 10-fold) of the cross section with increase in photon energy. Weik et al.³² have proposed the hot electron cascade mechanism to explain the wavelength dependence of the O₂ photodesorption from O₂ adsorbed on Pd(111) surface.

Photoabsorption by an evaporated Au film has been reported to be 64% at 360 nm and at normal incidence.³³ Although the absorption of Au(111) surface in the UV region is not available, it would be close to the evaporated-film value. Similar to Pd surfaces, photoelectron emission from an Au surface could not occur in the wavelength region of our present experiments, since the work function of Au is 5.3 eV, which corresponds to a photon wavelength of 234 nm. In addition, the formation of chemisorbed NO₂ results in an work function increase of 1.6 eV.¹⁰ The photoelectron tunneling from the Au surface to multilayer N₂O₄ may be responsible for the large cross section of multilayer N₂O₄ photodissociation. A change in the absorption by an evaporated Au film in the wavelength region from 250 to 400 nm is, however, so small (only a 9% increase³³) that the observed wavelength dependence of the cross section cannot be explained in terms of a simple photoelectron tunneling mechanism. Although the wavelength dependence could be ascribed to the hot electron cascade mechanism proposed by Weik et al.,³² as an alternative mechanism, we propose enhancement in the photoabsorption cross section of multilayer N₂O₄ by electron transfer from the substrate. A large increase in the work function upon NO₂ adsorption on Au(111) surface¹⁰ implies significant electron transfer from the substrate to chemisorbed NO₂. When NO₂ is adsorbed on chemisorbed NO₂, electron transfer would occur from chemisorbed NO₂ to multilayer N₂O₄. Such electron transfer could increase the photoabsorption cross section of multilayer N₂O₄. To determine whether direct absorption occurs or not, the polarization probe experiment is under preparation.

Sisk et al.³⁴ studied the dynamics of gas-phase N₂O₄ photolysis by a laser-induced fluorescence method and concluded that NO is not a primary photoproduct from the photodissociation channels of N₂O₄ at >300 nm. If the photodissociation process of multilayer N₂O₄ is similar to that of N₂O₄(g), then NO would not be a primary product but produced by the photodissociation of intermediate NO₂(ad). This mechanism is implausible for the NO photodesorption from multilayer N₂O₄. First, photodesorption of NO by this mechanism would depend quadratically on light intensity, if the cross section of NO₂(ad) is not so different from that of NO₂(g). Second, IRAS shows no formation of NO₂(ad) during the photolysis, because the stretching bands of NO₂ are strong enough to be detected even at coverages as low as 0.1 ML. Third, the electronic states of multilayer N₂O₄ are different from those of N₂O₄(g), as evidenced by the fact that the absorption spectrum of N₂O₄ adsorbed on LiF is quite different from that of N₂O₄(g). We assume, therefore, that N–O bond breaking occurs first in multilayer N₂O₄ photolysis to form N₂O₃, which undergoes spontaneous photodissociation to produce NO₂ and NO. Since the photodissociation cross section of adsorbed N₂O₃ is 1 order of magnitude greater than that of multilayer N₂O₄, the light intensity dependence is virtually linear in this case, and the

population of N₂O₃ during photolysis becomes too small to detect by IRAS.

Hasselbrink et al.² found that the NO yield is linear on laser fluence and the mean translational energy of the desorbing NO is independent of laser energy at 193, 248, 308, and 351 nm in the N₂O₄/NO/Pd(111) system. On the basis of these results, they speculated the formation of nitrosonium nitrate, NO⁺NO₃[−], in the dark, because this ionic form has often been observed in condensed N₂O₄ layers.^{20–23} If NO⁺NO₃[−] is present in adsorbed N₂O₄, neutralization of NO⁺ by electron capture would result in NO desorption with simultaneous tunnel back of an electron from NO₃[−] to the metal surface resulting in formation of NO₂. Givan and Lowenschuss²² reported that NO⁺NO₃[−] is produced upon temperature cycling only from less-ordered N₂O₄ layers, in which D-isomers are involved, but not from well-ordered N₂O₄(D_{2h}) layers. For our N₂O₄/NO₂/Au(111) system, IRAS showed clearly that multilayer N₂O₄ is dominantly ordered with the C₂ axis perpendicular to the surface. Furthermore, neither NO⁺NO₃[−] nor NO₃[−] was detected by IRAS before and during the photolysis. Failure in detecting NO⁺NO₃[−] due to insufficient sensitivity of IRAS can be ruled out, since NO⁺NO₃[−] has been detected by IRAS previously.^{20–23} Therefore, the concentration of NO⁺NO₃[−], if present, would be so small that it plays no important role in our system. It was also reported that matrix-isolated D-isomers are mainly converted into N₂O₄(D_{2h}) under illumination, but not to NO⁺NO₃[−].²⁵

In summary, multilayer N₂O₄ is photodecomposed to NO₂ and NO at <430 nm without formation of stable intermediates, while chemisorbed NO₂ and first-layer N₂O₄ undergo neither photodissociation nor photodesorption. The photodissociation cross section of multilayer N₂O₄ at 350 nm was determined to be 5.6 × 10^{−19} cm², which is close to the absorption cross section of gas-phase N₂O₄. The photodissociation on a water ice film was slower than that on the Au surface, suggesting that the photodissociation is enhanced by substrate excitation or by electron transfer from the surface to the adsorbates. The wavelength dependence of the cross section is very similar to the absorption spectrum of N₂O₄ adsorbed on LiF at 68 K. On the basis of these results, enhancement in the photoabsorption cross section of multilayer N₂O₄ by electron transfer from the substrate was proposed.

References and Notes

- (1) Zhou, X.-L.; Zhu, X.-Y.; White, J. M. *Surf. Sci. Rep.* **1991**, *13*, 73.
- (2) (a) Hasselbrink, E.; Jakubith, S.; Nettesheim, S.; Wolf, M.; Cassuto, A.; Ertle, G. *J. Chem. Phys.* **1990**, *92*, 3154. (b) Hasselbrink, E.; Nettesheim, S.; Wolf, M.; Cassuto, A.; Ertle, G. *Vacuum* **1990**, *41*, 287.
- (3) Dixon-Warren, St. J.; Jackson, R. C.; Polanyi, J. C.; Rieley, H.; Shapter, J. G.; Weiss, H. *J. Phys. Chem.* **1992**, *96*, 10983.
- (4) Solomon, S.; Garcia, R. R.; Rowland, F. S.; Wuebbles, D. J. *Nature* **1986**, *321*, 755.
- (5) Toon, O. B.; Turco, R. P. *Sci. Am.* **1991**, *264*, 68.
- (6) Toon, O. B.; Tolbert, M. A. *Nature* **1995**, *375*, 218.
- (7) Rieley, H.; McMurray, D. P.; Haq, S. J. *Chem. Soc., Faraday Trans.* **1996**, *92*, 933.
- (8) Rieley, H.; Colboy, J.; MacMurray, D. P.; Reeman, S. M. *J. Phys. Chem. B* **1997**, *101*, 4982.
- (9) Sato, S.; Suzuki, T. *J. Phys. Chem.* **1996**, *100*, 14769.
- (10) Bartram, M. E.; Koel, B. E. *Surf. Sci.* **1989**, *213*, 137.
- (11) Wang, J.; Koel, B. E. *J. Phys. Chem. A* **1998**, *102*, 8573.
- (12) Koch, T. G.; Horn, A. B.; Chesters, M. A.; McCoustra, M. R. S.; Sodeau, J. R. *J. Phys. Chem.* **1995**, *99*, 8362.
- (13) Greenler, R. G.; Rahn, R. R.; Schwartz, J. P. *J. Catal.* **1971**, *23*, 42.
- (14) Suetaka, W. *Surface Infrared and Raman Spectroscopy*; Plenum Press: New York, 1995; p 13.
- (15) Ibach, H.; Mills, D. L. *Electron Energy Loss Spectroscopy and Surface Vibrations*; Academic Press: New York, 1982.
- (16) Wiener, R. N.; Nixon, E. R. *J. Chem. Phys.* **1957**, *26*, 9.6.

- (17) Givan, A.; Loewenschuss, A.; *J. Chem. Phys.* **1990**, *93*, 866.
- (18) Fateley, W. G.; Bent, H. A.; Crawford, Jr., B. *J. Chem. Phys.* **1939**, *31*, 204.
- (19) Hisatsune, I. C.; Devlin, J. P.; Wada, Y. *J. Chem. Phys.* **1960**, *33*, 714.
- (20) Varette, E. L.; Pimentel, G. C. *J. Chem. Phys.* **1971**, *55*, 3813.
- (21) Givan, A.; Loewenschuss, A. *J. Chem. Phys.* **1989**, *90*, 6135.
- (22) Givan, A.; Loewenschuss, A. *J. Chem. Phys.* **1989**, *91*, 5126.
- (23) Givan, A.; Loewenschuss, A. *J. Chem. Phys.* **1990**, *93*, 7592.
- (24) Givan, A.; Loewenschuss, A. *J. Chem. Phys.* **1991**, *94*, 7562.
- (25) Bandow, H.; Akimoto, H.; Akiyama, S.; Tezuka, T. *Chem. Phys. Lett.* **1984**, *111*, 496.
- (26) Unpublished results.
- (27) Canning, N. D. S.; Outka, D.; Madix, R. J. *Surf. Sci.* **1984**, *141*, 240.
- (28) Hall, T. C.; Blacet, F. E. *J. Chem. Phys.* **1952**, *20*, 1745.
- (29) Johnston, H. S.; Graham, R. *Can. J. Chem.* **1974**, *52*, 1415.
- (30) Bach, W.; Breuer, H. D. *Discuss. Faraday Soc.* **1974**, *58*, 237.
- (31) Gilton, T. L.; Dehnhostel, C. P.; Cowin, J. P. *J. Chem. Phys.* **1989**, *91*, 1937.
- (32) Weik, F.; de Meijere, A.; Hasselbrink, E. *J. Chem. Phys.* **1993**, *99*, 682.
- (33) *Chronological Scientific Tables*; National Astronomical Observatory, Maruzen: Tokyo, 1997; p 521.
- (34) Sisk, W. N.; Miller, C. E.; Johnston, H. S. *J. Phys. Chem.* **1993**, *97*, 9916.